

A Two-Layered Wavelet-Based Algorithm for Efficient Lossless and Lossy Image Compression

Detlev Marpe, *Member, IEEE*, Gabi Blättermann, Jens Rieke, and Peter Maaß

Abstract—In this paper, we propose a wavelet-based image-coding scheme allowing lossless and lossy compression, simultaneously. Our two-layered approach utilizes the best of two worlds: it uses a highly performing wavelet-based or wavelet packet-based coding technique for lossy compression in the low bit range as a first stage. For the second (optional) stage, we extend the concept of reversible integer wavelet transforms to the more flexible class of adaptive reversible integer wavelet packet transforms which are based on the generation of a whole library of bases, from which the best representation for a given residue between the reconstructed lossy compressed image and the original image is chosen using a fast-search algorithm. We present experimental results demonstrating that our compression algorithm yields a rate-distortion performance similar or superior to the best currently published pure lossy still image-coding methods. At the same time, the lossless compression performance of our two-layered scheme is comparable to that of state-of-the-art pure lossless image-coding schemes. Compared to other combined lossy/lossless coding schemes such as the emerging JPEG-2000 still image-coding standard PSNR improvements up to 3 dB are achieved for a set of standard test images.

Index Terms—Best-basis algorithm, lossless image coding, lossy image compression, wavelet transform.

I. INTRODUCTION

IN THE past few years, wavelet-based methods have been successfully used for all sorts of lossy image compression. High coding efficiency, multiresolution image representation, and rather moderate computational complexity are the most striking attributes of these new methods. Current international standardization activities for still image coding (JPEG-2000 [1]) and for video coding (ITU-H.26L [3], MPEG-4 [4]) are under way, which are likely to incorporate various lossy coding techniques using wavelet transforms.

Lossless image compression, on the other hand, is still of some concern for special applications such as medical or satellite imaging where either legal or technical constraints exclude any loss of information. Algorithms for this type of image compression usually are based on predictive techniques in the spatial domain. The most efficient lossless image-coding

methods like CALIC [25] or JPEG-LS [23] rely on a sophisticated design of suitable predictors and of appropriate statistical models. However, recently a number of competitive lossless image-coding techniques using reversible integer wavelet transforms have been proposed [2], [11], [19], [27]. Among these new lossless image compression algorithms are some coding techniques, like S+P [19], CREW [27], and the JPEG-2000 image-coding system [2] which, in addition, allow lossy reconstructions out of an embedded organized bit-stream. This property along with the multiresolution nature of the underlying wavelet representation is useful especially for fast previewing of losslessly compressed images in archiving applications as well as for progressive transmission of image material in telemedical scenarios.

Although the combined lossless/lossy coding schemes have a lossless coding performance comparable to that of the best-known pure lossless schemes, they cannot compete with current state-of-the-art pure lossy still image coders. Our approach aims to bridge the gap in lossy coding performance between simultaneous lossy and lossless coding techniques, on the one hand, and pure lossy compression schemes on the other, while maintaining the same high performance in lossless coding mode as other lossless/lossy algorithms (like S+P). This objective is realized by using a two-layered approach. The first coding layer of our proposed algorithm uses an appropriately chosen biorthogonal wavelet or wavelet packet transform, uniform quantization and the (pre-)coding method of partitioning, aggregation, and conditional coding (PACC) [12]. In the second layer, the residue taken between the original image and its lossy reconstruction is coded using an adaptively chosen wavelet packet basis generated from an appropriately pre-defined integer wavelet kernel.

Our approach follows the observation that, in general, a single wavelet and its fixed related basis do not offer an optimal representation both with respect to lossy and lossless coding performance. In a recent study [6], it has been shown that other types of wavelets than the popular 9/7-tap biorthogonal filter [7] commonly used in lossy image compression systems show significantly better performance in lossless coding schemes such as S+P. Vice versa, the best losslessly performing integer wavelets do not yield a sufficiently high energy compaction to compete with state-of-the-art filter banks in the lossy domain. Thus, we draw the conclusion to break the coding process into two layers, where in each single layer, we have the freedom to choose an appropriate wavelet filter and/or basis representation.

The presented work is in the same spirit of so-called “lossy-plus-residual” methods, as proposed in [15], [22]. But, in contrast to these coding algorithms, our proposal is based on an efficient multiresolution representation, which

Manuscript received July 1999; revised April 2000. This paper was recommended by Guest Editor Y.-Q. Zhang.

D. Marpe and G. Blättermann are with the Image Processing Department, Heinrich-Hertz-Institute (HHI) for Communication Technology, Berlin, Germany.

J. Rieke is with the Department of Radiology, Charité, Humboldt-University, Berlin, Germany.

P. Maaß is with the Department of Mathematics, University of Bremen, Bremen, Germany.

Publisher Item Identifier S 1051-8215(00)08202-1.

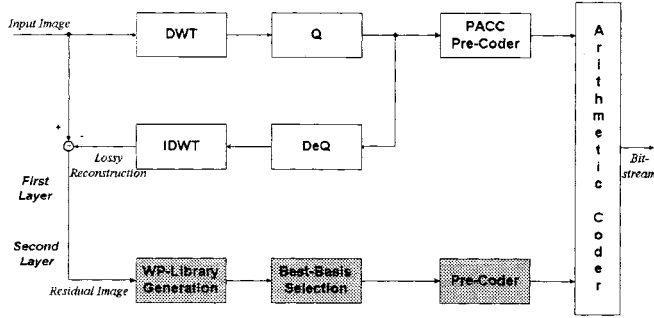


Fig. 1. Schematic representation of the proposed two-layered compression scheme (W/WP).

permits progressive transmission, decoding, and inspection by spatially scalable resolution. In addition, our algorithm is supplied with a built-in mechanism of adaptation to the user-defined switching point between the two coding layers, thus compensating to a large extent the main weakness of the aforementioned lossy-plus-residual methods, which consists in a strong dependency of the lossless compression performance on the quality of the lossy reconstruction.

This paper is organized as follows. In Section II, a brief overview of our proposed coding method is given. The key technique of adaptive wavelet packet transforms, and its realization with the help of fast search algorithms is the main topic of Section III. Section IV contains a detailed description of the lossy coding stage of our two-layered scheme with a special emphasis on a proposed method of adaptive dequantization which have not been published previously. The methods used to losslessly encode the residual image are discussed in Section V. In Section VI, we present simulation results for a comparison of our proposed algorithm with current state-of-the-art image-coding methods along with a brief discussion on some aspects regarding the computational complexity of our proposed method. Conclusions can be found in Section VII.

II. OVERVIEW OF THE PROPOSED IMAGE-CODING SYSTEM

In Fig. 1, a block diagram of our proposed two-layered compression scheme is given. The first layer, as depicted in the upper part of Fig. 1, consists of a discrete wavelet transform (DWT), a uniform quantizer (Q), and the PACC precoding module. A dequantization (DeQ) and a subsequent inverse DWT ($IDWT$) feed the second layer of the coding algorithm with a reconstructed image \hat{I} of the original image I . Given the residual image $R = I - \hat{I}$ and an appropriately chosen integer wavelet kernel, the second coding stage starts with the construction of an image-dependent library \mathcal{B} of wavelet packet bases. A fast search algorithm for the best basis $B^* \in \mathcal{B}$ provides an information cost minimizing representation of R , which is further processed in a pre-coding module and finally enters the arithmetic coder, where both the lossy and lossless part are multiplexed to a composite bit-stream.

In addition, we consider a variation of this two-layered scheme which has the same architecture, but where the lossy coding stage is also supplied with an adaptively chosen discrete wavelet packet transform ($DWPT$). To distinguish this latter scheme from the former one, we introduce the notation

W/WP for the two-layered approach with a fixed wavelet (W) representation in the lossy coding layer and an adaptively chosen wavelet packet (WP) basis in the lossless coding stage, whereas the scheme operating with an adaptive wavelet packet transform in both the lossy and lossless coding stage is denoted by WP/WP .

III. THE BEST-BASIS FRAMEWORK

In this section, we first give a brief review of the concept of adaptive wavelet packet representation using the best-basis algorithm. We further outline a Lagrangian optimization technique which is useful in the context of lossy WP-based image coding, and finally introduce a simplified realization of this powerful technique.

A. Wavelet Packet Representation and Best-Basis Search Algorithms

Given an input image I and a wavelet kernel, *i.e.*, a pair of low- and high-pass filters (H, G), the construction of a library of separable wavelet, packet bases is performed by iterated application of (H, G) on rows and columns of I , subsequently [26]. At each iteration step, four subbands are generated out of a given subband $W_{l,k}$ according to the recursive relation¹

$$W_{l,k} = W_{l+1,4k} \oplus W_{l+1,4k+1} \oplus W_{l+1,4k+2} \oplus W_{l+1,4k+3} \quad (1)$$

where $0 \leq l \leq L$ and $0 \leq k < 4^l$. The collection of all subband decompositions of I for a given maximum decomposition level L forms a full balanced quadtree of depth L , where each subtree covering the root corresponds to a so-called wavelet packet basis. Thus, we have a one-to-one correspondence between the full depth- L quadtree of subbands of a given image I and a library of WP-bases $\mathcal{B}_L(I)$. The standard wavelet basis which is related to an octave band tree generated by an iterative decomposition of the low-pass band $W_{l,0}$ is, for instance, a particular member of this library.

Due to the tree structure of the WP library $\mathcal{B}_L = \mathcal{B}_L(I)$, a fast search for the best representation in the sense of minimum information cost is feasible. Provided that an information cost-functional M operating on \mathcal{B}_L is given, such that M is additive in the sense that the cost of four child nodes equals the sum of the costs of each of the four children, the so-called *best basis* $B^* \in \mathcal{B}_L$ of a given image I is obtained by traversing the quadtree from the leaves to the root and by applying the following “divide-and-conquer” rule at each node: *if the sum of the cost of the four child nodes is greater than or equal to the cost of the parent, prune the part of the tree below the parent node, otherwise assign the children’s cost to the parent node* [8], [26].

This algorithm introduced by Coifman and Wickerhauser [8] is a powerful tool for the generation of an appropriate representation of signals with *a-priori* unknown spectral properties. Residual images obtained as quantization error images with strongly differing quality of the base layer reconstruction belong to this type of signals. This observation leads to the idea of constructing a WP library based on an appropriately chosen

¹In a mathematical rigorous sense this relation holds only for an orthogonal filter bank (H, G)

integer wavelet kernel, such that the best-basis approach is applicable to lossless residual image coding. In Section V, a more detailed description of a concrete realization of that idea will be given.

Regarding lossy image-coding applications, the standard wavelet basis has proven to be well suited for most natural images. Since this image class is characterized by a mixture of a strong low-frequency energy component with well-localized high-frequency energy components, the low-pass branched subtree related to the wavelet basis is, in general, a good fit to that kind of signal characteristics. For some individual images with specific spatial frequency characteristics however, there are better-suited representations within a given WP library which, in principle, can be chosen adaptively by using the best-basis algorithm [14], [26].

However, operating on unquantized WP coefficients the originally proposed best-basis search algorithm does not properly reflect the rate-distortion (R-D) dependencies inherently given in a lossy image-coding scenario. To overcome this drawback, Ramchandran and Vetterli [16] proposed to use a Lagrangian optimization technique where both the quantization and the WP basis are jointly optimized. Given a WP library \mathcal{B}_L and an admissible set \mathcal{Q} of quantizers, each combination of WP transform and quantizer results in a (R, D) point in the global operational R-D plane, so that the underlying optimization problem considered in [16] consists in selecting the best among those achievable (R, D) points which meet a given bit-rate constraint. A classical well-known solution to this problem is the Lagrangian optimization technique which converts the given optimization problem into an unconstrained problem by introducing a Lagrange factor $\lambda \geq 0$

$$J^*(\lambda) = \min_{B \in \mathcal{B}_L, Q \in \mathcal{Q}} (J(\lambda) = D + \lambda \cdot R).$$

Although the algorithm proposed in [16] exploits the tree structure of \mathcal{B}_L according to the orthogonality relation of (1) with the same fast “divide-and-conquer” strategy as the original best-basis search algorithm, it is computationally much more demanding due to the consideration of \mathcal{Q} quantizer decisions at each node and due to the iterative way of searching for the optimal Lagrangian factor.

B. A Fast Nearly Optimal WP Basis Search Algorithm

In [5], we recently presented a much simplified and yet highly efficient variation of a best-basis search algorithm operating in a R-D optimal sense. First, we found experimentally that using more than one fixed overall uniform quantization method (like that presented in Section IV-A) for all subbands yields only marginal gains. Thus, we dropped these additional degrees of freedom in the optimization algorithm originally proposed in [16]. Given a fixed quantizer, we further evaluated whether there exists a relation between the chosen quantization step sizes and the optimal Lagrangian factor for a representative image class. For this purpose we have performed a set of R-D measurements where the Lagrangian factors were fixed and the quantization step sizes were changed. This experimental evaluation resulted in a specification of *one fixed Lagrange factor* λ_{opt} independent

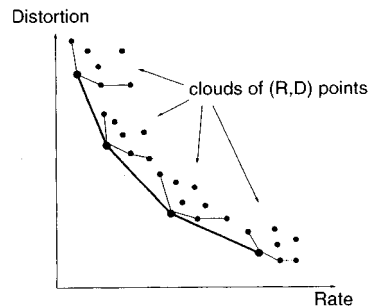


Fig. 2. Convex hull of all achievable (R, D) points.

of the chosen quantization parameter, which allows us to detect nearly all optimal (R, D) points on the convex hull of the clouds of all achievable (R, D) point (cf. Fig. 2).

Summarizing our finding is a fast search algorithm for the (nearly) optimal WP basis in the R-D sense can be given as follows.

- 1) Expand a given image I in the WP library \mathcal{B}_L .
- 2) Quantize each WP coefficient according to the given step size and dead zone.
- 3) Evaluate the Lagrangian $J_{l,k}$ cost of each quantized subband $\hat{W}_{l,k}$, *i.e.*,

$$J_{l,k} \stackrel{\text{def}}{=} J(\hat{W}_{l,k}) = D(\hat{W}_{l,k}) + \lambda_{\text{opt}} \cdot R(\hat{W}_{l,k}).$$

- 4) Compare the cost $J_{l,k}$ of each node (l, k) with sum of the costs of its four children $J_{l,k}^{\text{child}} \stackrel{\text{def}}{=} \sum_{j=0}^3 J_{l+1, 4k+j}$ by traversing the tree bottom-up (for $l \leq L-1$). If $J_{l,k}^{\text{child}}$ is greater or equal to the cost $J_{l,k}$ of the parent, prune the part of the tree below the node (l, k) ; otherwise, assign $J_{l,k}^{\text{child}}$ to $J_{l,k}$.
- 5) Choose the WP basis related to the leaves of the final pruned tree as the best WP basis of the image I .

We would like to add some remarks concerning the choice of appropriate measures of rate $R(\cdot)$ and distortion $D(\cdot)$.

If, for example, a mean-squared error (MSE) minimizing strategy is followed, the sum of squared error (SSE) representing the error energy may be an appropriate candidate of an additive distortion measure. Note, however, that in the case of using a biorthogonal filter kernel for the generation of the WP library \mathcal{B}_L , the orthogonality condition given by (1) is only valid in an approximative sense, so that the MSE in the spatial domain may differ from the (weighted) sum of each SSE measurement obtained on the individual subbands of the best-basis representation.

Moreover, most practical choices of a rate measure R admit only rough estimations of the real achievable bit-rate (e.g., given by the first-order entropy) unless each subband belonging to the whole tree would have been encoded prior to the Lagrangian cost evaluation, which would be computationally too expensive and hence impracticable.

However, these problems do not impose any serious limitations on the practical usability of this algorithm, as long as the employed measures reflect the *relative* distance of the nodes in the WP tree. In fact, our comparative evaluation of different cost functions did not demonstrate any significant differences in

performance, so that the one with the least computational complexity may be chosen [5].

IV. THE LOSSY CODING LAYER

The lossy or “base” coding layer of our proposed two-layered scheme is a conventionally structured transform coding scheme consisting of a fixed wavelet or, alternatively, an adaptively chosen wavelet packet transform, a simple uniform scalar quantizer, and the PACC coder (cf. Fig. 1).

Since the previous section already provides a detailed description of the transform part, we concentrate in this section on taking a closer look at the two remaining building blocks of the lossy coding layer of our proposed scheme.

A. Uniform Quantization and Adaptive Context-Based Selection of Reconstruction Values

In our coding approach, we use a simple uniform scalar quantization of the wavelet (packet) coefficients with an overall step size Δ and a dead-zone, *i.e.*, a larger zero bin $[-\tau, \tau]$, where the ratio $\eta = (2\tau/\Delta) = 1.5$ has been chosen empirically. Assuming that the high-resolution quantization hypothesis holds outside the zero bin, which is in turn a justification of the approximate optimality of this type of quantizer design [9], it is a reasonable choice to select the midpoint of each bin as the reconstruction value. However, a careful analysis of the probability density function (pdf) $p(x) = p_{l,k}(x)$ of wavelet (packet) coefficients reveals that $p(x)$ has some variations, especially in bins close to the zero bin and for wavelet (packet) coefficients in a high-frequency subband $W_{l,k}$ with low decomposition level l .

Thus, we propose a simple but yet efficient mechanism to adapt the reconstruction value to the varying distribution of wavelet coefficients. Instead of modeling a given distribution $p(x)$ with the help of a set of pdf models [21], we use a piecewise linear approximation of $p(x)$ to determine the (nearly) optimal reconstruction value in a MSE-minimizing sense. For a given quantization bin $[u_n, u_{n+1}]$ and pdf $p(x)$, the MSE-optimal reconstruction value r_n is determined by the centroid condition

$$r_n = \frac{\int_{u_n}^{u_{n+1}} xp(x) dx}{\int_{u_n}^{u_{n+1}} p(x) dx}. \quad (2)$$

Given the empirical distribution, *i.e.*, the (normalized) histogram $h(x)$ of the wavelet coefficients, we define the piecewise linear interpolating pdf $\bar{p}(x) \stackrel{\text{def}}{=} ((h_{n+1} - h_n)/\Delta)(x - u_n) + h_n$, where $u_{n+1} - u_n = \Delta$ and $h(x) = h_n$ for all $x \in [u_n, u_{n+1}]$.² Evaluating (2) with $\bar{p}(x)$ instead of $p(x)$, we get an approximation \bar{r}_n of the MSE-optimal reconstruction value r_n by

$$\bar{r}_n = u_n + \frac{2h_{n+1} + h_n}{3(h_{n+1} + h_n)} \Delta. \quad (3)$$

For flat parts of a given distribution with $h_{n+1} \approx h_n$, the sub-optimal reconstruction value \bar{r}_n is close to the midpoint recon-

²Note that $\bar{p}(x)$ is only defined outside the zero bin $[-\tau, \tau]$. Assuming a symmetric pdf, we further restrict our analysis to the interval $[\tau, \infty)$.

TABLE I
RATE (BPP) VERSUS PSNR (dB) OBTAINED BY DIFFERENT METHODS OF DEQUANTIZATION FOR THE *LENA* IMAGE

Rate	Dequant. Using Trained Codewords	Adaptive Context-Based Dequant.	Dequant. Using Midpoints
1.0	40.76	40.72	40.54
0.5	37.64	37.62	37.52
0.25	34.64	34.62	34.54
0.125	31.66	31.64	31.57

struction value, as expected. But for highly peaked areas of a pdf $p(x)$ with $h_{n+1} \ll h_n$, which can be observed in real measured densities of wavelet coefficients in the neighborhood of $x = 0$, (3) determines a reconstruction value \bar{r}_n which moves from the midpoint toward zero thereby approaching u_n , the left-hand side of the quantization bin.

An experimental evaluation of the proposed adaptive choice of reconstruction values has been performed using a set of standard grayscale test images. Table I shows some characteristic results comparing the performance of our proposed method with that of the simple choice of midpoint reconstruction values, on the one hand, and the theoretical limit of the ideal case given by trained reconstruction values, on the other hand.³ For that purpose, (optimal) codewords have been trained on unquantized wavelet coefficients by computing for each subband mean values of those coefficients which were mapped to a given individual quantization bin.

Note that our proposed method implies that the dequantizer has to build histograms of all (decoded) quantization levels prior to dequantization. To further improve the proposed reconstruction algorithm, we incorporate the context information for magnitudes of quantization levels (see Section IV-B below). Thus, we divide each histogram into eight sub-histograms according to the classification given by the context states and compute a separate reconstruction value for each context state.

The results given in Table I show that our method of adaptive context-based reconstruction performs very close to the ideal reconstruction using trained codewords for each context state. However, the coding gain compared to a dequantization using simple midpoint reconstruction values is rather small (up to 0.2-dB PSNR). But since the proposed dequantization method also improves the performance of the subsequent lossless coding layer, it is worth the marginal overhead in computational complexity.

B. Pre-Coding Methods for the Lossy Compression Stage

The lossy coding stage is built around the conceptual ideas presented in [12]. We give a brief review of the underlying coding strategy; for more details, the reader is referred to [12], [13].

PACC pre-coding is a three-stage process. An initial *partitioning* process splits the quantized wavelet representation into three sub-sources: the *significance map* indicating the position

³Note that the rates given for the system operating with trained codewords are no real bit rates since they do not include the number of bits necessary for transmitting the codeword values.

of significant coefficients, the *magnitude map* holding the absolute values of significant coefficients, and the *sign map* with the phase information of the wavelet coefficients. Note that all three sub-sources inherit the subband structure from the wavelet (packet) decomposition, which induces an additional partition of each sub-source.

In a second (optional) step, an *aggregation* of insignificant coefficients across different scales is performed using a quadtree related data structure. This well-known instrument of zerotree-coding [20] connects insignificant coefficients which share the same spatial location in the octaveband structured multiresolution analysis. However, in contrast to other methods using zerotrees, we only consider zerotree roots localized in subbands on the maximum decomposition level which guarantee a sufficient coding benefit.

The final *conditioning* stage of the PACC pre-coding method supplies the elements of each sub-source with a *context*, *i.e.*, an appropriate model for the actual coding process in the adaptive arithmetic coder. For coding of the significance maps, appropriate conditioning contexts have been created with the help of heuristically designed prototype templates. These templates consist of a causal scale and orientation-dependent neighborhood of the actual coding event. In the case of a standard wavelet basis, the templates cover additional causally accessible information represented by the neighbors of the parent and/or by the sisters of the actual coding event with respect to the siblings relationship of the (standard) wavelet decomposition. Processing of quantized coefficients is performed band-wise and in the order of lowest to highest frequency bands, such that the significance information is coded (and decoded) first.

This allows the construction of special conditioning states for coding of the magnitude of a significant coefficient by using the local significance information of the coefficient's 8-neighborhood. Thus, the conditioning context state $\kappa = \kappa(c)$ of a given coefficient c in a subband is given by sum of two terms $\kappa = \kappa^{(1)} + \kappa^{(2)}$, where $\kappa^{(1)}$ is simply the sum of the significance states of the vertical and horizontal neighbors and where $\kappa^{(2)}$ maps the significance states of the four diagonal neighbors on three different states. This results in eight different context states for the coding of magnitudes.

Finally, for the conditional coding of sign maps, a higher order Markov model is used, whose states are built of two preceding sign events of a given coefficient with respect to the orientation of the related subband.

Encoding of the lowest frequency subband (LL-band) in the low-pass branch of a decomposition tree is done by using a DPCM-like procedure with an adaptive median predictor [10] and a classification of the prediction error with a five-state context model.

V. RESIDUAL CODING LAYER

In order to achieve an optional lossless reconstruction of a given image, the quantization error of the lossy coding layer or its equivalent in the spatial domain, the residual image has to be encoded losslessly by a second coding layer, the so-called *residual coding layer*.

TABLE II
LOSSLESS CODING RATE (BPP) VERSUS BASIS SELECTION FOR DIFFERENT RESIDUAL REPRESENTATION AT VARIOUS LOSSY BIT-RATES

Basis selection	Rate of lossy reconstruction				
	2.0	1.0	0.5	0.25	0.125
$\mathbf{W}_{0,0}$	3.88	3.92	4.30	4.74	5.28
$\mathbf{W}_{1,0} \oplus \mathbf{W}_{1,1} \oplus \mathbf{W}_{1,2} \oplus \mathbf{W}_{1,3}$	3.98	3.73	3.75	3.81	3.95
Best Basis of $\mathcal{B}_3(R)$	3.88	3.73	3.75	3.78	3.87

A. Wavelet Packet Representation of the Residual Image

Depending on the quality of the lossy reconstruction, the residue taken between the original and reconstructed image contains more or less strong correlations, which may not be efficiently captured by a fixed wavelet basis. Thus, we follow the strategy of first generating a whole library of wavelet packet bases which, in a second step, can be used to select adaptively an appropriate basis.

Unlike other image-coding algorithms based upon the best-basis algorithm [14], [16], we propose to use this framework in a scenario, where the underlying WP-libraries are generated by integer wavelet kernels. Integer wavelets permit reversible integer representations of a given image, and, in addition, allow fast implementations using a lifting factorization [6].

As an illustration of how the concept of adapted waveforms will cope with the given problem, let us consider the typical phenomenon that with increasing quality of the lossy reconstruction, the residual image R tends to loose its coherence and, at some point, mainly consists of uncorrelated noise. Since the construction of the WP library $\mathcal{B}_L(R)$ includes the original spatial-domain representation $\mathbf{W}_{0,0}$ of R as the root of the corresponding depth- L quadtree, the search algorithm may choose $\mathbf{W}_{0,0}$ as the best representation⁴ for a noisy residue in the case of a high-quality lossy reconstruction. Table II provides real measured lossless coding rates⁵ of a given image depending on different bit rates of the embedded lossy coded part. These coding results have been obtained by using two fixed bases, namely $\mathbf{W}_{0,0}$ and the level-1 decomposition $\mathbf{W}_{1,0} \oplus \mathbf{W}_{1,1} \oplus \mathbf{W}_{1,2} \oplus \mathbf{W}_{1,3}$, on the one hand, and the best basis of a depth-3 WP-library $\mathcal{B}_3(R)$, on the other hand. As indicated by the numbers, $\mathbf{W}_{0,0}$ is chosen as the best basis at a lossy rate of 2 bpp, where a nearly perfect reconstruction is achieved. At lower rates of the lossy coded image, e.g., 0.5 and 1 bpp, the level-1 basis is selected as the optimal representation. Given a very low bit-rate reconstruction of the lossy coded original image, the two candidates of representations are no longer optimal for the resulting residual image, so that a best-basis selection from the larger depth-3 library $\mathcal{B}_3(R)$ results in overall lower coding rates (cf. Table II).

B. Pre-Coding Techniques for the Residual Coding Layer

Statistical modeling of wavelet coefficients obviously relies on assumptions which are confined to a certain scope of applicability. Thus, we propose a re-design of the PACC pre-coding method serving the needs of the residual coding stage.

⁴For mathematical convenience, we use the notation of subband decomposition and WP basis synonymously.

⁵Note that the (negligible) overhead of one bit per quadtree node to determine the chosen WP basis has been included.

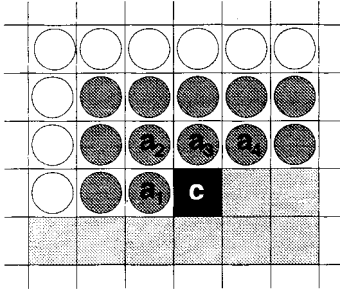


Fig. 3. Neighborhood used to encode a residual coefficient c . The coefficients lying in the past of the coding event c are marked with a circle; the shaded circles are those neighboring coefficients, which contribute to the context decision for the magnitude coding of c . a_1, \dots, a_4 defines the template used for coding of the significance state of c .

Two major modifications have been employed. First, we found, that, given a residual representation consisting of predominant high-frequency information, it is no longer useful to perform a zerotree aggregation. This is mainly due to the fact that, in general, the residual image contains most of the image noise which results in nonvanishing wavelet coefficients on small scales. Besides that, an arbitrary WP-basis different from the octave-band decomposition no longer offers a natural parent-child relationship between coefficients on different scales.

The second modification of the PACC pre-coding technique for its application in the residual coding stage concerns an appropriate re-design of conditioning contexts especially for the coding of significance and magnitude maps created by the initial partitioning process (cf. Section IV-B).

For the coding of significance information, we propose a band-independent template given by the four nearest causal neighbors a_1, \dots, a_4 of the actual coding event c , as depicted in Fig. 3. However, in contrast to the lossy case, the significance map does not provide enough information of the local variance for a proper design of conditioning states for the magnitudes of residual wavelet coefficients. Thus, we propose to classify the magnitude of an actual coefficient c according to the weighted sum $\hat{\sigma}(c)$ of the variances $\sigma(a_1), \dots, \sigma(a_4)$ of the neighboring coefficients a_1, \dots, a_4

$$\hat{\sigma}(c) \stackrel{\text{def}}{=} w_1\sigma(a_1) + w_2\sigma(a_2) + w_3\sigma(a_3) + w_4\sigma(a_4),$$

where $\sum_{j=1}^4 w_j = 1$. The variances $\sigma(a_i)$ are obtained by using an intersection of a 3×3 -window centered at the corresponding neighbor a_i , with the set of coefficients already visited in the past of the actual coding event c . In Fig. 3, the 12 neighboring coefficients of c contributing to the calculation of $\hat{\sigma}(c)$ are shown as gray shaded circles.

The actual classification is finally obtained by using a backward adaptive uniform quantization of the actual variance prediction $\hat{\sigma}(c)$ according to an estimation of the mean value $\bar{\varsigma}_N$ of the variance prediction values of all $N - 1$ preceding coefficients c_1, \dots, c_{N-1} of c and that of $c_N \stackrel{\text{def}}{=} c$ itself

$$\bar{\varsigma}_N = \frac{\sum_{i=1}^N \hat{\sigma}(c_i)}{N}$$

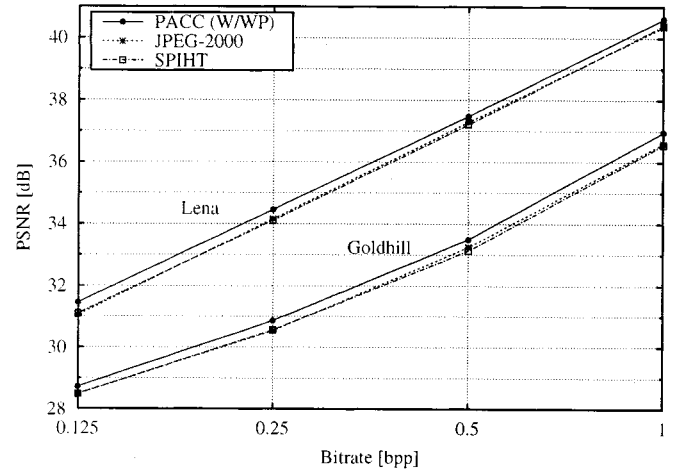


Fig. 4. R-D performance of lossy/lossless PACC (W/WP) coding scheme in comparison with pure lossy coding schemes.

such that the actual context $\iota(c)$ for the coding of $|c|$ is given by

$$\iota(c) = \min \left(\left\lfloor \frac{4 \cdot \hat{\sigma}(c)}{\bar{\varsigma}_N} \right\rfloor, 7 \right)$$

where $\lfloor x \rfloor$ denotes the greatest integer less than or equal to x . This definition leads to a separation into eight different context states for conditional coding of the magnitude map, which was found experimentally to yield best overall performance.

VI. EXPERIMENTAL RESULTS AND DISCUSSION

In this section, we present simulation results using the proposed two-layered coding scheme. Three sets of experiments were carried out in order to demonstrate the performance of our proposed approach relative to other relevant schemes. First, we evaluate the R-D performance of the lossy base layer. The lossless coding performance and its dependency on the lossy coding rates is the subject of the second evaluation. Finally, we present a performance comparison of our proposed scheme with other combined lossy/lossless image-coding methods, where in addition to a set of standard images, some typical medical images have been used for benchmarking. A brief discussion of some aspects concerning the computational complexity of the proposed method concludes this section.

A. R-D Performance of the Lossy Coding Layer

The first set of experiments aims at evaluating the rate distortion performance of our proposed scheme in comparison with pure lossy algorithms. For that purpose, we employed a four-level standard wavelet transform generated by the biorthogonal 9/7-tapped filter bank [7] in the lossy coding layer. As a measure of distortion, the PSNR was used. All results were generated from decoded bit streams.

Fig. 4 shows R-D-curves for the *Lena* and *Goldhill* image both with 512×512 pixels and 8 bits/pixel. As reference schemes, we used the pure lossy coding scheme of JPEG-2000 VM⁶ (Version 6.0) [2] in single layer mode (with default parameters) and the widely regarded standard reference SPIHT-coder

⁶Verification Model.

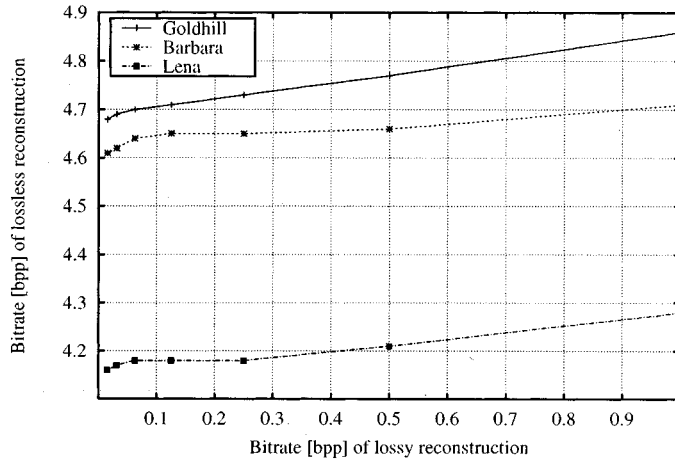


Fig. 5. Lossless coding performance vs. lossy coding rates obtained by PACC (W/WP) for three 512×512 standard gray-scale images.

of Said and Pearlman [18]. For a fair comparison, both reference coders were supplied with the same 9/7 biorthogonal filter bank as our lossy coding layer. First, it is interesting to note that the JPEG-2000 and the SPIHIT coder have virtually the same objective performance, although they are quite different from an algorithmic point of view. While the latter is based on hierarchical trees, thereby exploiting the parent-child relationship of the dyadic decomposition [18], the former ignores interband relationships and uses independently coded blocks in the subband domain, such that the bit-stream contribution of each code block is determined in a post-compression R-D optimization process [2].

Regarding the performance of the lossy coding layer of our proposed scheme, we observe some small advantages in PSNR of 0.2–0.5 dB in favor of our proposed PACC scheme (cf. Fig. 4). Note, however, that both reference schemes do not permit a lossless reconstruction, at least not in the lossy coding mode, that we considered for this kind of performance evaluation.

B. Lossless Coding Performance

In the following, we summarize the outcome of our experiments concerning the lossless compression performance of our combined scheme. The experiments were based on an implementation of our proposed method using the lossy coding layer as described in the previous Section VI-A and by choosing the integer wavelet kernel (4, 4) [6] for the generation of a depth-3 WP-library in the residual coding layer.

Fig. 5 shows the results of our coding simulation regarding the dependencies of lossy and residual coding rates. It can be observed that the lossless coding performance given by the total bit rate deteriorates from lower to higher bit rates of the (embedded) lossy coded part, as expected. But the difference in measured lossless bit-rates over the whole interval of interesting lossy bit-rates is confined to a variance of $\pm 2\%$ relative to the average of all measured lossless rates.

For a comparison with other combined lossless/lossy and pure lossless coding schemes, we computed the mean value of measured lossless bit-rates in the lossy coding range of 0.125–1 bpp for each of the three standard grayscale images

TABLE III
LOSSLESS CODING RATES (BPP) OBTAINED BY DIFFERENT COMBINED LOSSLESS/LOSSY AND PURE LOSSLESS CODING SCHEMES

Coding scheme		<i>Lena</i>	<i>Barbara</i>	<i>Goldhill</i>
PACC	W/WP	4.21	4.66	4.76
	WP/WP	4.22	4.58	4.76
S+P		4.20	4.71	4.78
JPEG-2000		4.32	4.79	4.84
JPEG-LS		4.24	4.86	4.71
CALIC		4.12	4.63	4.63

Lena, *Barbara*, and *Goldhill* ($512 \times 512 \times 8b$). In addition, we considered in this experiment a variation of the lossy coding layer, which uses our fast nearly optimal WP basis search algorithm (cf. Section III-B) on a depth-3 WP library generated by the 9/7 biorthogonal wavelet kernel and which we denote by WP/WP in distinction from the scheme with a (fixed) wavelet-based lossy coding layer (W/WP).

As reference schemes, we used in the category of pure lossless operating coding methods two of the best performing schemes,⁷ the CALIC-coder [25] and the lossless coding standard JPEG-LS [23]. In the group of combined lossy/lossless coding schemes, the reversible coding method of JPEG-2000 [2] (with default settings) and the S+P-scheme [19] were used.

Table III shows the simulation results of our comparative investigations. The proposed PACC-coder produces lossless rates exceeding those of the best performing schemes by, at most, 2%–3%; in one case, it even outperforms the best pure lossless schemes. In addition, if pure lossless performance is the primary goal, our scheme is capable of approaching the best obtainable lossless bit-rates in the limit of diminishing lossy rates, as can be observed from the results plotted in Fig. 5. The lossless coding performance of the W/WP and WP/WP scheme is quite similar; for the *Barbara* image, however, there is a small gain due to the prominent (lossy) coding efficiency of wavelet packets on this kind of image material (cf. the following section).

C. Performance Comparison of Combined Lossy/Lossless Schemes

In our third and final part of simulation experiments, we compared our coding approach to the combined lossy/lossless coding reference schemes JPEG-2000 (J2K) and S+P. Notice that both reference schemes were operating with a fixed integer wavelet for both lossless and lossy coding. In order to emphasize the advantage of our proposed two-layered coding scheme concerning the selection of an appropriate filterbank for the lossy coding stage, we employed a recently proposed 22/14-tapped biorthogonal coiflet [24] with slightly better R-D-performance than the 9/7-tapped wavelet system in the lossy coding layer.

The coding results given in Table IV show that compared to the reference schemes our proposed method achieves a significant PSNR gain of 0.6–3.3 dB on the set of three standard images. Coding gains obtained by the adaptive wavelet packet based lossy coding layer (WP/WP) relative to its wavelet-based

⁷At least to the best of our knowledge.

TABLE IV
RATE (BPP) VERSUS PSNR [dB] OBTAINED BY LOSSY/LOSSLESS CODING
SCHEMES FOR A SET OF STANDARD IMAGES

Image	Rate	S+P	J2K	PACC	
				W/WP	WP/WP
<i>Lena</i>	1.0	39.44	39.30	40.72	40.68
	0.5	36.52	36.35	37.62	37.61
	0.25	33.63	33.29	34.62	34.62
	0.125	30.81	30.30	31.64	31.43
<i>Barbara</i>	1.0	35.53	35.84	37.65	38.37
	0.5	30.57	30.93	32.75	33.87
	0.25	26.89	27.39	28.78	30.09
	0.125	24.46	24.76	25.64	26.97
<i>Gold-hill</i>	1.0	35.80	35.96	37.05	37.10
	0.5	32.60	32.76	33.56	33.61
	0.25	30.23	30.16	30.89	31.01
	0.125	28.21	28.18	28.80	28.83

variant (W/WP) are up to 1.3 dB. However, for the *Lena* image, the PACC-WP/WP scheme shows a slightly worse objective performance compared to its counterpart W/WP. This stems from the facts that the WP library in the lossy coding layer was restricted to the depth of three levels, and in the WP/WP scheme, no zerotree aggregation was performed.

Finally, we evaluated the three combined lossy/lossless coding schemes on a more application oriented test set of three medical images: a chest radiograph *CR* ($1568 \times 1968 \times 10b$), a magnetic resonance image *MR* ($256 \times 256 \times 11b$), and a computed tomography image *CT* ($512 \times 512 \times 12b$). The results given in Table V show that in terms of PSNR, our proposed coding scheme achieves a distinguished gain up to 3.3 dB compared to the reference schemes. However, it should be noted that a gain in PSNR does not necessarily correlate with an increase in diagnostic quality; typically, methods using receiver operator characteristic (ROC) curves are used to evaluate the impact of (different) compression methods on the diagnostic accuracy [17]. As shown in Table VI, the lossless rates obtained by the proposed two-layered algorithm on the given medical images are comparable to those rates measured for S+P and JPEG-2000 VM, the latter in default lossless mode.

D. Considerations of Computational Complexity Issues

In this section, we address some aspects concerning the computational complexity of our presented approach. At the encoder, the computational complexity is mainly increased by the reconstruction loop and by employing an additional adaptive WP transform when compared to the reference schemes with combined lossy/lossless coding mode. Note however, that this only affects the optional lossless coding mode; the computational complexity of the lossy coding layer, both at the encoder and decoder, is comparable to that of the reference schemes, at least in the case of using the standard wavelet transform in this layer where, of course, the actual complexity may depend on the chosen wavelet filter.

Regarding the computational complexity of the best-basis methods involved in the adaptive WP transforms, we proposed in a previous work [14] a modification of the original best-basis

TABLE V
RATE (BPP) VERSUS PSNR (dB) OBTAINED BY LOSSY/LOSSLESS
SCHEMES FOR A SET OF MEDICAL IMAGES

Image	Rate	S+P	J2K	PACC
				W/WP
<i>CR</i>	1.0	54.47	54.89	56.44
	0.5	52.37	52.56	53.66
	0.25	50.28	50.84	51.88
<i>CT</i>	1.0	61.22	60.56	63.83
	0.5	54.10	53.14	56.29
	0.25	47.57	46.58	49.50
<i>MR</i>	1.0	47.36	46.79	48.20
	0.5	43.03	42.17	43.91
	0.25	39.13	38.24	40.03

TABLE VI
LOSSLESS COMPRESSION RESULTS (BPP) ON MEDICAL IMAGES
FOR COMBINED LOSSLESS/LOSSY CODING SCHEMES

Image	S+P	J2K	PACC
			W/WP
<i>CR</i>	3.59	3.61	3.53
<i>CT</i>	3.80	3.91	3.77
<i>MR</i>	5.82	5.96	5.83

approach, the so-called *complexity-constrained best-basis* algorithm, which offers an instrument for complexity scalability in the sense that it allows to control the trade-off between R-D performance and computational complexity by a single parameter. This objective is achieved by generating a restricted WP library depending on a given complexity budget, where the way the library is restricted depends on the given signal and its energy distribution. For a more detailed discussion on that issue, the reader is referred to [14]. Besides there is the possibility to restrict the WP library in advance. For the residual coding layer we can reduce the number of admissible WP bases drastically, and hence, decrease the computational complexity by up to a factor of two if, for example, the switching point between both layers is known *a priori*.

VII. CONCLUSION

We presented a novel wavelet-based image-coding scheme that provides lossy and lossless recovery simultaneously. In order to jointly optimize the performance of both coding modes, we propose to divide the coding process into two layers. The first coding layer is based on a DWT or, alternatively, on an adaptively chosen wavelet packet transform generated by an appropriately chosen wavelet filter kernel for good energy compaction and decorrelation. Coupled with the PACC coding strategy, this first coding stage performs a lossy compression with high efficiency in a R-D sense. In the second layer, the residual image is decorrelated using an adaptive wavelet packet integer transform along with some suitable techniques for the statistical coding of transform coefficients. Our experimental results demonstrate that our proposed method achieves a performance similar or superior to the best currently published

image compression algorithms either of the pure lossless, pure lossy, or combined lossy/lossless type.

REFERENCES

- [1] *Coding of Still Pictures, Call for Contributions for JPEG 2000 Image Coding System*, ISO/IEC JTC 1/SC 29/WG 1, Doc. N 505, Mar. 1997.
- [2] *JPEG 2000 verification model version 6.0*, ISO/IEC JTC 1/SC 29/WG 1, Doc. N 1575, Jan. 2000.
- [3] ITU-T, Study Group 16, "Call for proposals for H.26L video coding," Question 15/16, Geneva, Switzerland, Jan. 1997.
- [4] "Special Issue on MPEG 4," *IEEE Trans. Circuits Syst. Video Technol.*, vol. 7, Feb. 1997.
- [5] G. Blättermann, D. Marpe, and H. L. Cycon, "Fast optimal basis selection for wavelet packet-based adaptive image compression," in *Proc. MATHTOOLS'99*, St. Petersburg, Russia, 1999.
- [6] A. Calderbank *et al.*, "Lossless image compression using integer to integer wavelet transforms," Dept. of Math., Princeton Univ., Princeton, NJ, Tech. Rep., Sep. 1996.
- [7] A. Cohen, I. Daubechies, and J.-C. Feauveau, "Biorthogonal bases of compactly supported wavelets," *Commun. Pure Appl. Math.*, vol. 45, pp. 485–560, 1992.
- [8] R. R. Coifman and M. V. Wickerhauser, "Entropy-based algorithms for best-basis selection," *IEEE Trans. Inform. Theory*, vol. 38, pp. 713–718, Feb. 1992.
- [9] S. Mallat and F. Falzon, "Analysis of low bit rate image transform coding," *IEEE Trans. Signal Processing*, 1998.
- [10] S. A. Martucci, "Reversible compression of HDTV images using median adaptive prediction and arithmetic coding," in *Proc. Symp. Circuits and Systems*, 1990, pp. 1310–1313.
- [11] N. Memon, X. Wu, and B.-L. Yeo, "Entropy coding techniques for lossless image compression with reversible integer wavelet transforms," IBM Res. Rep., Yorktown Heights, NY, Oct. 1997.
- [12] D. Marpe and H. L. Cycon, "Efficient pre-coding techniques for wavelet-based image compression," in *Proc. PCS 1997*, Berlin, Germany, 1997, pp. 45–50.
- [13] —, "Very low bit-rate video coding using wavelet-based techniques," *IEEE Trans. Circuits Syst. Video Technol.*, vol. 9, pp. 85–94, Feb. 1999.
- [14] D. Marpe, H. L. Cycon, and W. Li, "A complexity constrained best-basis wavelet packet algorithm for image compression," *Proc. Inst. Electr. Eng.—Visual, Image, and Signal Processing*, vol. 145, no. 6, Dec. 1998.
- [15] M. Rabbani and P. W. Melnychuk, "Conditioning contexts for the arithmetic coding of bit planes," *IEEE Trans. Signal Processing*, vol. 40, pp. 232–236, Jan. 1992.
- [16] K. Ramchandran and M. Vetterli, "Best wavelet packet bases in a rate-distortion sense," *IEEE Trans. Image Processing*, vol. 2, pp. 160–175, Apr. 1993.
- [17] J. Rieke, P. Maaß, E. L. Lopez Hänninen, T. Liebig, H. Amthauer, C. Stroszczyński, W. Schauer, T. Boskamp, and M. Wolf, "Wavelet versus JPEG and fractal compression: Impact on the detection of low-contrast details in computed radiographs," *Invest. Radiol.*, vol. 33, pp. 456–463, 1998.
- [18] A. Said and W. A. Pearlman, "A new fast and efficient image codec based on set partitioning in hierarchical trees," *IEEE Trans. Circuits Syst. Video Technol.*, vol. 6, pp. 243–250, June 1996.
- [19] —, "An image multiresolution representation for lossless and lossy compression," *IEEE Trans. Image Processing*, vol. 5, pp. 1303–1310, Sept. 1996.
- [20] J. M. Shapiro, "Embedded image coding using zerotrees of wavelet coefficients," *IEEE Trans. Signal Processing*, vol. 41, pp. 3445–3462, Dec. 1993.
- [21] T. Strutz and E. Müller, "Image data compression with pdf-adaptive reconstruction of wavelet coefficients," *Proc. SPIE*, vol. 2569, pp. 747–758, 1995.
- [22] S. Takamura and M. Takagi, "Lossless image compression with lossy image using adaptive prediction and arithmetic coding," in *IEEE Proc. Data Compression Conf. (DCC)*, Mar. 1994, pp. 166–174.
- [23] M. J. Weinberger, G. Seroussi, and G. Sapiro, "LOCO-I: A low complexity, context-based lossless image compression algorithm," in *IEEE Proc. Data Compression Conf. (DCC)*, 1996, pp. 140–149.
- [24] D. Wei, H.-T. Pai, and A. C. Bovik, "Antisymmetric biorthogonal coflet for image coding," to be published.
- [25] X. Wu and N. Memon, "Context-based, adaptive lossless image coding," *IEEE Trans. Commun.*, vol. 45, pp. 437–444, Apr. 1997.
- [26] M. V. Wickerhauser, *Adapted Wavelet Analysis From Theory to Software*. Wellesley, MA: A. K. Peters, 1994.
- [27] A. Zandhi *et al.*, "CREW: Compression with reversible embedded wavelets," in *IEEE Proc. Data Compression Conf. (DCC)*, 1995, pp. 212–221.



Detlev Marpe (M'00) received the Dipl. Math. degree (with highest honors) from the Technical University of Berlin (TUB), Berlin, Germany, in 1990.

During 1991–1993, he was a Research and Teaching Assistant in the Department of Mathematics, TUB. Since 1994, he has been involved in several industrial and research projects in the area of still image coding and very low bit-rate video coding. Since 1999, he has been with the Image Processing Department, Heinrich-Hertz-Institute (HHI) for Communication Technology, Berlin, Germany. His current research interests include wavelet theory, still image and video coding, image analysis, and information theory. He is an active member of ITU-T Study Group 16, Question 15.



Gabi Blättermann received the Dipl. Math. degree from the University of Applied Sciences (TFH), Berlin, Germany, in 1998. She is currently working toward the Ph.D. degree at the University of Rostock, Rostock, Germany, supported by the Hypatia program at TFH.

She joined the Image Processing Department of Heinrich-Hertz-Institute (HHI), Berlin, Germany, in 1999. Her current research interests include wavelet-based coding for still image and video coding, in particular scalable coding methods.

Ms. Blättermann received the Tiburtius-Price for her diploma thesis on image coding in 1999.



Jens Rieke was born in 1965. He graduated from University of Düsseldorf Medical School in 1992.

He is a member of staff in the Department of Radiology, Charité University Hospital, Berlin, Germany, and since 1999, has also been Head of the Digital Radiology Working Group. His research interests and scientific publications range from telemedical applications and their impact on clinical workflow, to imaging and interventional procedures in oncology.



Peter Maaß received the Dipl. Math. from the University of Heidelberg, Heidelberg, Germany, in 1985, and the Ph.D. degree from the Technical University of Berlin, Berlin, Germany, in 1988. Additionally, he studied mathematics at both the Technical University of Karlsruhe, Karlsruhe, Germany, and Pembroke College, Cambridge, U.K.

From 1990 to 1991, he was an Assistant Professor at Tufts University, Boston, MA, and from 1991 to 1993, an Assistant at the University of Saarbrücken, Saarbrücken, Germany. From 1993 to 1999, he was a Full Professor of Mathematics at the University of Potsdam, Potsdam, Germany. Currently, he is a Professor of Mathematics at the University of Bremen, Bremen, Germany, where he is Director of the Center of Technomathematics. The emphasis of his research is applied functional analysis, especially wavelet analysis and inverse problems.